Techno-Science Research Journal 5 (2017) 48-54

Content list available at ITC

Techno-Science Research Journal

Journal Homepage : www.itc.edu.kh

Techno-Science Research Journal

Estimation of Discontinuous Systems using Receding-horizon Unscented Kalman Filter

Sarot Srang and Masaki Yamakita

Institute of Technology of Cambodia, Russian Ferderation Blvd., P.O. Box 86, Phnom Penh, Cambodia.

Abstract: *Discontinuous systems have been increasingly paid attention since they can be found ranging from physical to biological systems. In this paper we consider an effective estimation algorithm for systems with discontinuous vector field. We propose an incorporation between the existing recedinghorizon nonlinear Kalman filter (RNKF) and the unscented transformation, which is named receding-horizon unscented Kalman filter (RUKF). The use of unscented transformation is beneficial to discontinuous systems since it does not require partial derivatives as does the linearization technique which may incur severeness at discontinuity. An application of this algorithm to a system with discontinuous friction is considered to illustrate its performance in comparison with the classical unscented Kalman filter (UKF).*

1. INTRODUCTION

With great challenge in engineering problems and echnologies, many researchers increasingly pay attention on discontinuous systems which are widely seen ranging from physical to biological systems, such as system with friction [1], dynamical network with switching topology [2], and iological neural networks [3]. Due to highly nonlinear property on discontinuity, there are significant problems such as inaccurate computation (chattering) and various types of trajectory behavior which cannot be handled by using classical analysis like Lipschitz functions. There are riches of analysis on semistability, multistability and bifurcation in the form of differential inclusion using Filippov's convex method, [2], [3]. However, estimation of the prescribed systems has not been widely investigated. In our paper, we account for stochastic model for such systems and estimationproblems are considered.

Kalman filter and extended Kalman filter (EKF) are very powerful approaches as they have been applied to various advanced engineering problems for more than three decades. Because EKF is applied to nonlinear systems, it has been widely used for prediction, navigation systems, adaptive control, robust control, system identification and many other areas [4]. Despite its usefulness, many researchers have tried to find other nonlinear filtering approach. [5] proposed unscented Kalman filter (UKF). It has, later, been roved more robust than EKF in several cases [6]. In addition, it can incorporate highly nonlinear systems including system with discontinuous vector field since the propagation of prediction can be done via unscented transform which is derivative free.

Based on continuous-time limit with respect to time step, [7] derived continuous-time unscented Kalman filter, later called unscented Kalman-Bucy filter (UKBF) and analyzed by [8], and derived continuous-discrete unscented Kalman filter (CDUKF). In addition, the latter one is proved to outperform discrete UKF by showing simulation result of reentry vehicle tracking problem. In our previous work, it was successfully applied to highly uncertain systems with multiple discontinuities [9]. In this work, we consider a control system with uncertain model of discontinuous friction as in [9]. We propose an estimation algorithm incorporating the existing receding-horizon nonlinear Kalman (RNKF) [10] with unscented transformation, which is called "recedinghorizon unscented Kalman filter (RUKF)". The central idea of RNKF is based on augmented state in the horizon interval, and, thus, it is able to handle systems with constraints. For linear unconstrained systems, it was shown that the current estimate is the result of Kalman filter and the other previous estimates are the result of optimal smoothing. [11] gave the general fixed-lag smoother which employed Rauch-Tung-Striebel smoother equations. The difference from the RNKF and RUKF is that the smoothed estimates are computed after all the Kalman filter estimates are known. [12] also proposed an algorithm for the same purpose. However, the algorithm is given in a creative way, but not based on principle.

This paper is organized as follows. In the next section, we investigate behavior of chattering around sliding surface, and we bring up an approach of Filippov's convex method to obtain accurate computation when state variable orbits along sliding surface. In Section 3, we will point out the problem formulation of discrete time filtering, and we introduce the formulation of RUKF algorithm. To show the robustness of the algorithm, numerical simulation results and discussions

This work was not supported by any organization.
S. Srang and M. Yamakita are with Department of echanical and Control Systems Engineering, Tokyo Institute of Technology, 2-12-1 Ookayama, Meguro-ku, Tokyo, Japan 152-8552
srangsarot@ac.ctrl.titech.ac.jp or
yamakita@ac.ctrl.titech.ac.jp

of an application example is given in Section 4. We sum up our work in Section 5.

2. COMPUTATION OF FILIPPOV SYSTEM

In this section, we will specifically investigate computational behavior of a dynamical system where the vector field involves discontinuities. We illustrate the existence of chattering if we use conventional method to compute the corresponding discretized system, and we also give a solution to avoid chattering by approximately define average vector field around discontinuities using Filippov's convex method. This section, therefore, deals with numerical method to improve accuracy of computation which is independent from the estimation algorithm presented in the rest of the paper.

2.1. *Chattering*

Consider a state equation of a deterministic system following,

$$\dot{x}(t) = f(x,t) \tag{1}$$

where $x \in \mathbb{R}^n$, and $f(x,t)$ is discontinuous vector field. Let Σ be a set of discontinuity surface described by a scalar smooth function $\sigma(x)$. Then it is defined by $\Sigma = \{x \in \mathbb{R}^n \mid \sigma(x) = 0\}$.

A discontinuity surface that the system state of (1) orbits along is called sliding surface. Numerically, chatteringaround the surface is incurred, which is illustrated in Fig. 1. Chattering of one dimensional system is studied by [13]. In this paper, we investigate namely trajectory error due to chattering for n-dimensional system using Euler method whose computation induces largest error in comparison with Rung-Kutta and other numerical integration methods. Euler approximation of (1) is, then, written as

$$x_{k+1} = x_k + f(x_k, t_k)\Delta t \tag{2}$$

where Δt is sampling time.

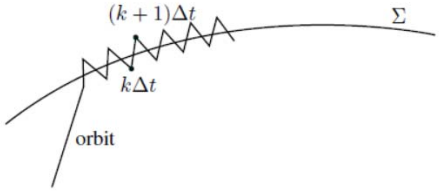

Fig. 1. Orbit of state along sliding surface

Suppose that (1) has continuum equilibria along sliding surface, i. e. $f(x_s,t) = 0$ for $x_s \in \Sigma$. Then, the system state, theoretically, reaches the continuum equilibria in finite time for any $x_0 \in \mathbb{R}^n$ [13], [14]. For (2), assume that a right sampling time $\Delta t'$ is selected in such way that at time $k^*\Delta t'$, the state x_{k^*} reaches the surface Σ. Then, we obtain $f(x_{k^*}, t_{k^*}) = 0$, and thus

$$x_{k^*+1} = x_{k^*}, \tag{3}$$

which means that the computational state never leaves the surface once it reaches, and, hence, it does not generate trajectory error. However, in practice, we never find the right sampling time, so the computational state does not reach the surface, but instead, it bounces around the surface.

Consider trajectory error $\epsilon(x_p)$ around a sliding surface Σ, which is generated by neighborhood $x_p \in \mathcal{B}_\delta(x_s)$, where $x_s \in \Sigma$ and δ is positive. We, thus, have $f(x_p,\tau) \neq 0$, where τ is corresponding time at which computational state of (2) becomes x_p. We define

$$\begin{aligned} \epsilon(x_p) &= \sigma(x_{p+1}) \\ &= \sigma(x_p + f(x_p,\tau)\Delta t). \end{aligned} \tag{4}$$

It is often the case to consider that maximum trajectory error around a sliding surface can be defined by

$$\epsilon_{\max} = \sup_{x_s \in \Sigma} \left(\sup_{\tau > 0} \sup_{x_i \to x_s} |\sigma(x_i + f(x_i,\tau)\Delta t)| \right) \tag{5}$$

if Δt is small enough, and $f(x,\tau)$ is smooth for $x \in \mathcal{B}_\delta(x_s)$ except its center. For autonomous system, $f(x,t) = f(x)$, then (5) becomes

$$\epsilon_{\max} = \sup_{x_s \in \Sigma} \left(\sup_{x_i \to x_s} |\sigma(x_i + f(x_i)\Delta t)| \right). \tag{6}$$

2.2. *Filippov Approach*

For the vector field of the dynamical system (1), assume that there are N discontinuity surfaces Σ_i described by N scalar smooth functions $\sigma_i(x)$. Then the vector field can be rewritten as [15],

$$f(x,t) = f_{\text{orig}}(x,t) + \sum_{i=1}^{N} \Delta_i(x,t)\mu_i(x) \tag{7}$$

where

$$\mu_i(x) = \begin{cases} 1, & \sigma_i(x) > 0, \\ [0,1], & \sigma_i(x) = 0, \\ 0, & \sigma_i(x) < 0. \end{cases} \tag{8}$$

The introduced base vector field $f_{\text{orig}}(x,t)$ is defined from the vector field when $\sigma_i(x) < 0$ for all i, and the individually additional term $\Delta_i(x,t)$ can, then, be defined using the condition $\sigma_i(x) > 0$ in (8).

The introduced base vector field $f_{\text{orig}}(x,t)$ is defined from the vector field when $\sigma_i(x) < 0$ for all i, and the individually additional term $\Delta_i(x,t)$ can, then, be defined using the condition $\sigma_i(x) > 0$ in (8).

To define $\mu_i(x)$ when the system (1) is sliding, we must consider that the system state may orbit along two or more sliding surfaces simultaneously. Let S be a set of index

of sliding surface along which the system state orbits and N_S be total element number of S. Then the condition $\frac{\partial \sigma_i(x)}{\partial x} f(x,t) = 0$ for $i \in S$ must hold. By using (7), this condition can be elaborated as

$$\frac{\partial \sigma_i(x)}{\partial x} f_{\text{orig}}(x,t) + \frac{\partial \sigma_i(x)}{\partial x} \sum_{k=1}^{N} \Delta_k(x,t)\mu_k(x) = 0. \quad (9)$$

Denote

$$\{\alpha_1, \ldots, \alpha_{N_S}\} = \{\mu_i(x)\}, \quad \{\beta_1, \ldots, \beta_{N_S}\} = \{\sigma_i(x)\}$$
$$\{\gamma_1, \ldots, \gamma_{N_S}\} = \{\Delta_i(x,t)\} \quad (10)$$

for $i \in S$. From (9) and (10), we obtain

$$\begin{bmatrix} \alpha_1 \\ \vdots \\ \alpha_{N_S} \end{bmatrix} = \begin{bmatrix} \frac{\partial \beta_1}{\partial x}\gamma_1 & \cdots & \frac{\partial \beta_1}{\partial x}\gamma_{N_S} \\ \vdots & \cdots & \vdots \\ \frac{\partial \beta_{N_S}}{\partial x}\gamma_1 & \cdots & \frac{\partial \beta_{N_S}}{\partial x}\gamma_{N_S} \end{bmatrix}^{-1} \times \begin{bmatrix} \frac{\partial \beta_1}{\partial x}\widetilde{f}(x,t) \\ \vdots \\ \frac{\partial \beta_{N_S}}{\partial x}\widetilde{f}(x,t) \end{bmatrix}, \quad (11)$$

where

$$\widetilde{f}(x,t) = f_{\text{orig}}(x,t) + \sum_{k \in \{N \setminus S\}} \Delta_k(x,t) \frac{\text{sign}(\sigma_k(x)) + 1}{2}.$$

It is considered that $\mu_i(x)$ defined by (10) and (11) may satisfy $\mu_i(x) \notin [0,1]$ which means that the system state is not constrained to the i^{th} discontinuity surface. Denote $S' = \{i \in S \mid \mu_i(x) \notin [0,1]\}$. Thus, (7) can be rewritten as

$$f(x,t) = f_{\text{orig}}(x,t) + \sum_{i \in \{N \setminus S\}} \Delta_i(x,t) \frac{\text{sign}(\sigma_i(x)) + 1}{2} + \sum_{i \in \{S \setminus S'\}} \Delta_i(x,t)\mu_i(x) + \sum_{i \in S'} \Delta_i(x,t) \frac{\text{sign}(\mu_i(x))}{2} \quad (12)$$

For computation of system involving discontinuity, chattering always occurs around sliding surface since the system state never reaches any sliding surface in finite time, as explained in the previous subsection. In order to improve computational accuracy, we define an interval for sliding surface as $|\sigma_i(x)| < \epsilon_i$, where ϵ_i is a threshold which is computed by (5) or (6); and a term of attraction to the sliding surface is added to the average vector field defined in (12). Therefore, approximation of average vector field can be written as

$$f(x,t) = f_{\text{orig}}(x,t) + \sum_{i \in \{N \setminus S\}} \Delta_i(x,t) \frac{\text{sign}(\sigma_i(x)) + 1}{2} + \sum_{i \in \{S \setminus S'\}} \Delta_i(x,t)\mu_i(x) + \sum_{i \in S'} \Delta_i(x,t) \frac{\text{sign}(\mu_i(x)) + 1}{2} - \sum_{i \in \{S \setminus S'\}} C_i \sigma_i(x) \left(\frac{\partial \sigma_i(x)}{\partial x} \right)^T, \quad (13)$$

where C_i is positive if the condition $|\sigma_i(x)| < \epsilon_i$ is satisfied; and it is zero otherwise.

3. RECEDING-HORIZON UNSCENTED KALMAN FILTER

In most practical applications, state equation of a dynamical system is stochastically modeled as

$$\dot{x}(t) = f(x,t) + e(t) \quad (14)$$

where $x(t) \in \mathbb{R}^n$ is state; $e(t)$ is white Gaussian noise; and $f(x,t)$ is called drift function, which is discontinuous. The solution of the differential equation (14) is however continuous. This equation can be discretized as

$$x_{k+1} = x_k + \int_{k\Delta t}^{(k+1)\Delta t} f(x,t)dt + v_k = F(x_k, t_k) + v_k \quad (15)$$

where v_k is Gaussian noise with known covariance matrix Q. The accuracy of (15) can be assured if the selected Δt is small, and the stability of estimation can be improved by using extra additive process covariance, ΔQ (see [8]). The general measurement equation is modeled in discrete time as

$$y_{k+1} = H(x_{k+1}) + w_k \quad (16)$$

where $y \in \mathbb{R}^p$ is measurement, H is measurement model function and w_k is measurement noise assumed to be Gaussian with known covariance matrix R.

Recently, [10] introduced the RNKF in which the Kalman filtering framework is extended to include a receding horizon in an optimization framework. The time update of this algorithm, however, engages linearization which is not compatible with discontinuous systems. We propose a receding-horizon unscented Kalman filter which incorporates the receding horizon framework with unscented transformation as follows.

Initialization Step

The same as RNKF, RUKF starts after a window of h measurements are obtained. At any time instant k, denote $m_{k-h|k-h}$ and $P_{k-h|k-h}$ as mean and corresponding covariance matrix respectively, both of which are assumed available. The first estimation problem is solved at time $k = h$, and it, thus, requires initialized mean and covariance at time $k = 0$, which are denoted as x_0 and P_0 respectively. For the time $k = 1, \ldots, h$, the estimates can be obtained with variable window sizes accordingly.

Let n_h be the number of augmented state over a window size h. Then $n_h = nh$, and the associated weights for sigma points corresponding to the augmented state are defined as following

$$W_0^{(m_h)} = \frac{\lambda_h}{n_h + \lambda_h}$$

$$
\begin{aligned}
W_0^{(c_h)} &= \frac{\lambda_h}{n_h+\lambda_n} + (1-\alpha^2+\beta) \\
W_i^{(m_h)} &= \frac{1}{2(n_h+\lambda_h)}, \quad i = 1,\ldots,2n_h \\
W_i^{(c_h)} &= \frac{1}{2(n_h+\lambda_h)}, \quad i = 1,\ldots,2n_h
\end{aligned} \tag{17}
$$

where $\lambda_h = \alpha^2(n_h+\kappa) - n_h$. The positive constants α, β and κ are the unscented Kalman filter parameters. For ease of reading, we will present our whole algorithm in matrix form to calculate mean, covariance and cross-covariance matrices, which are associated with the following weight matrices,

$$
\begin{aligned}
w_{m_h} &= \left[W_0^{(m_h)} \cdots W_0^{(m_h)}\right] \\
W_h &= (I - [w_{m_h} \cdots w_{m_h}]) \begin{bmatrix} W_0^{(c_h)} & & \\ & \ddots & \\ & & W_{2n_h}^{(c_h)} \end{bmatrix} \\
&\quad \times (I - [w_{m_h} \cdots w_{m_h}])^T,
\end{aligned} \tag{18}
$$

These weight matrices are used to compute mean and covariance from the sample sigma points, where the full explanation can be found in [7].

Time Update Step

Let us consider the time update of the state estimation over window size h, starting from filtered estimates at time k. Denote $m_{k|k}$ and $P_{k|k}$ be *a posteriori* of the mean and its error covariance matrix at time k respectively, both of which are available. The predicted estimates for all the states in the time interval $[k+1, k+h]$ are obtained by the 'open loop' propagation of sigma points via the state equation (15). The propagated sigma points are augmented as

$$
X^a_{k+h|k} = \left[X^T_{k+h|k}(k+1) \cdots X^T_{k+h|k}(k+h)\right]^T, \tag{19}
$$

and the augmented mean corresponding the augmented sigma point is denoted as

$$
m^a_{k+h|k} = \left[m^T_{k+h|k}(k+1) \cdots m^T_{k+h|k}(k+h)\right]^T. \tag{20}
$$

Then the predicted covariance matrix of the augmented states $P^a_{k+h|k}$ at the time $(k+h)^{th}$ is defined by

$$
P^a_{k+h|k} = \begin{bmatrix} P^{n\times n}_{k+h|k}(k+1,k+1) & \cdots & P^{n\times n}_{k+h|k}(k+1,k+h) \\ P^{n\times n}_{k+h|k}(k+2,k+1) & \cdots & P^{n\times n}_{k+h|k}(k+2,k+h) \\ \vdots & \ddots & \vdots \\ P^{n\times n}_{k+h|k}(k+h,k+1) & \cdots & P^{n\times n}_{k+h|k}(k+h,k+h) \end{bmatrix} \tag{21}
$$

The block diagonal matrices of (21) represent the error covariance matrices in the open loop state estimates, whereas the off-diagonal matrices are the cross-covariance between the open loop state estimation errors at different time instants.

All the block elements of $X^a_{k+h|k}$, $m^a_{k+h|k}$ and $P^a_{k+h|k} \in \mathbb{R}^{nh\times nh}$ defined in (19) to (21) are computed using unscented transformation. The i^{th} element of $X^a_{k+h|k}$ and $m^a_{k+h|k}$ are respectively calculated by the followings,

$$
\begin{aligned}
X_{k+h|k}(i-1) &= [m_{k+h|k}(i-1) \cdots m_{k+h|k}(i-1)] \\
&\quad + \sqrt{c_1}\left[0 \quad \sqrt{P_{k+h|k}(i-1)} \quad -\sqrt{P_{k+h|k}(i-1)}\right] \\
X_{k+h|k}(i) &= F\left(X_{k+h|k}(i-1), t_{k+i-1}\right), \quad \text{and} \\
m_{k+h|k}(i) &= X_{k+h|k}(i) w_{m_1}.
\end{aligned} \tag{22}
$$

where $c_1 = n_1 + \lambda_1$ and F is the propagated function defined in (15). Then, the ii^{th} diagonal block element of $P^a_{k+h|k}$ is calculated along with the i^{th} element of $X^a_{k+h|k}$ as

$$
P^a_{k+h|k}(i,i) = X_{k+h|k}(i) W_1 X^T_{k+h|k}(i) + Q. \tag{23}
$$

The upper triangle element of $P^a_{k+h|k}$, i.e. $P^a_{k+h|k}(i,j)$ where $i<j$, is defined by

$$
P^a_{k+h|k}(i,j) = X_{k+h|k}(i) W_1 X^T_{k+h|k}(j) \tag{24}
$$

The complete upper triangular blocks of $P^a_{k+h|k}$ can now be calculated with these recursive relationships when the first block $P^a_{k+h|k}(1,1)$ is initialized with

$$
P^a_{k+h|k}(1,1) = X_{k|k} W_1 X^T_{k|k} + Q. \tag{25}
$$

where $X_{k|k}$ is defined in terms of $m_{k|k}$ and $P_{k|k}$ by the formulation of the first equation in (22). Since $P^a_{k+h|k}$ is symmetric, the lower triangle blocks are the transpose of the upper ones.

Measurement Update Step

The predicted estimates of the augmented states are updated using all the measurements in the time window [k + 1; k + h] based on, again, unscented transformation.

$$
y^a_{k+h} = \left[y^T(k+1) \cdots y^T(k+h)\right]^T. \tag{26}
$$

Then the complete measurement update is as the follows

$$
\begin{aligned}
\mathcal{X}^a &= \left[m^a_{k+h|k} \cdots m^a_{k+h|k}\right] \\
&\quad + \sqrt{c_h}\left[0 \quad \sqrt{P^a_{k+h|k}} \quad -\sqrt{P^a_{k+h|k}}\right] \\
&= \left[\mathcal{X}_1^T \cdots \mathcal{X}_h^T\right]^T \\
\mathcal{Y}^a_{k+h|k} &= \left[H(\mathcal{X}_1)^T \cdots H(\mathcal{X}_h)^T\right]^T \\
y^a_{k+h|k} &= \mathcal{Y}^a_{k+h|k} w_{m_h} \\
P^a_{yy} &= \mathcal{Y}^a_{k+h|k} W_h \mathcal{Y}^{aT}_{k+h|k} + R^a \\
P^a_{xy} &= \mathcal{X}^a_{k+h|k} W_h \mathcal{Y}^{aT}_{k+h|k} \\
K^a &= P^a_{xy} P^{a\ -1}_{yy} \\
m^a_{k+h|k+h} &= m^a_{k+h|k} + K^a(y^a_{k+h} - y^a_{k+h|k})
\end{aligned} \tag{27, 28}
$$

$$P^a_{k+h|k+h} = P^a_{k+h|k} - K^a P^a_{yy} K^{aT}$$

where R^a is given by $\text{diag}(R^{p\times p} \dots R^{p\times p})$.

4. APPLICATION TO FRICTION ESTIMATION FOR ADAPTIVE CONTROL

In this paper, we consider an adaptive compensation of static friction which is modeled as

,

$$F_f = (\alpha_0 + \alpha_1 e^{-(\omega/\omega_s)^2})\text{sign}(\omega) + \alpha_2\omega, \qquad (29)$$

where ω is angular velocity; ω_s is Stribeck velocity; $\alpha_0+\alpha_1$ is static friction; α_0 is Coulomb friction; and α_2 is coefficient of viscous friction. We use the algorithm in Section 3 to estimate the friction from a model of DC motor as following,

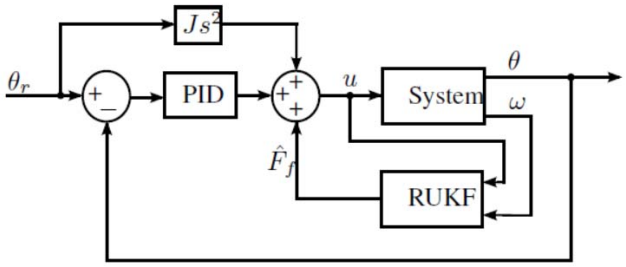

Fig. 2. Block diagram of adaptive control

$$\dot{\omega}(t) = \frac{1}{J}[-\text{sign}(\omega), -e^{-(\omega/\omega_s)^2}\text{sign}(\omega), -\omega]\alpha + \frac{u}{J} \qquad (30)$$

where $\alpha = [\alpha_0, \alpha_1, \alpha_2]^T$, J is the total moment of inertia of the motor and u is control torque, and $\Phi(\omega) = 1/J[-\text{sign}(\omega), -e^{-(\omega/\omega_s)^2}\text{sign}(\omega), -\omega]$ is called basis function.

We simulate a control system which is illustrated by the block diagram in Fig. 2. The desired position is $\theta_r(t) = 2.8\sin(0.02\pi t)\sin(2\pi t)$ whose shape is indicated in Fig. 3, and our simulation is run up to 400 seconds. All the friction parameters used for our simulation are obtained from [16]. The augmented state and parameter to be estimated is $x = [\omega(t) \quad \alpha]^T$. We consider the case in which $\omega_s = 2.4$, but we simulate our system in two difference cases.

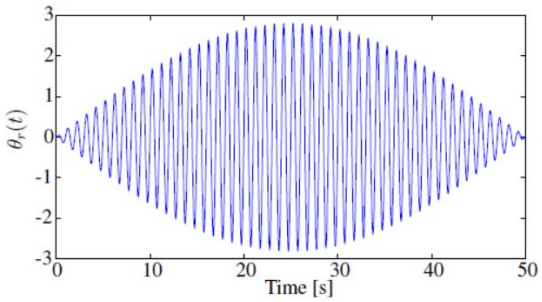

Fig. 3. Tracking reference

First, we use unbiased basis function which means that we choose the same ωs = 2:4 for estimator. The performance of tracking control obtained from using both UKF and RUKF is shown in Fig. 4. It indicates that tracking error using UKF is larger, especially at low velocity, (around 0, 50 and 100 seconds, the trajectory in Fig. 3 has small amplitude, and so does the velocity). This is because the parameters of frication are not well estimated, as shown in Fig. 5. On sliding surface (at zero velocity), the system was shown unobservable by [9], and, therefore, both estimations diverge. However, convergence can be recovered when velocity is away from zero. Fig. 5 indicates that parameter estimationnusing RUKF is less sensitive than using UKF because, like RNKF, RUKF has the optimal smoothing property.

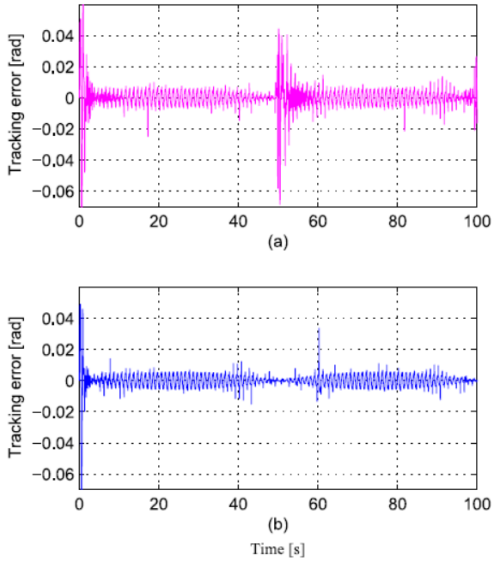

Fig. 4. Tracking performance for unbiased model: (a) using UKF and (b) using RUKF with $h = 4$

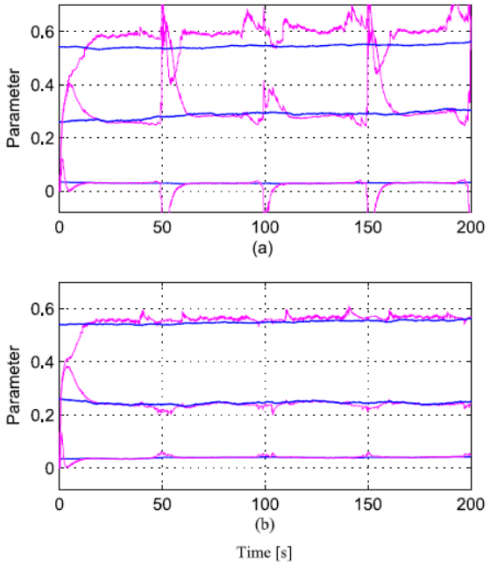

Fig. 5. Parameter estimation for unbiased model: actual (blue) and estimate (pink); (a) using UKF and (b) using RUKF

Second, we select $\omega_s = 0.01$ for estimation algorithm, meaning that biased basis function is used, as considered in [9]. The temporal evolutions of estimated parameters, $\hat{\alpha}(t) = [\hat{\alpha}_0 \quad \hat{\alpha}_1 \quad \hat{\alpha}_2]^T$, are no longer constant, which are illustrated by estimation result in Fig. 6 and 7. The parameters, $\hat{\alpha}_0$ and $\hat{\alpha}_2$ have fairly periodic form over 50 seconds which is the haft period of $\sin(0.02\pi t)$, so that we only show them over the last period. Whereas, the parameter $\hat{\alpha}_1$ seems to reach the steady state after about 70 seconds. The results of friction estimation and tracking error are shown in Fig. 8 and 9 respectively. Compared to the result using UKF, the performance of using RUKF is slightly better as indicated in Fig. 9.

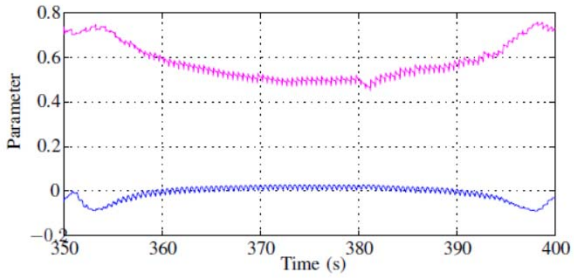

Fig. 6. Time-evolution of parameter ($h = 4$): $\hat{\alpha}_0$ (pink) and $\hat{\alpha}_2$ (blue)

5. CONCLUSIONS

To handle estimation problem of discontinuous systems, in this paper computational accuracy around discontinuity surface of a discretized system is investigated, and Filippov's approach is used to improve the computational accuracy for such systems. Moreover, we propose an estimation algorithm, receding-horizon unscented Kalman filter which extends the framework of the existing receding-horizon nonlinear Kalman filter incorporated with unscented transformation.

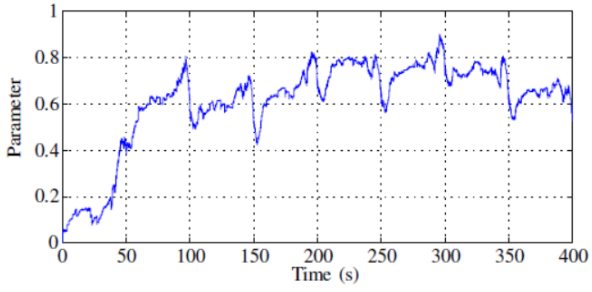

Fig. 7. Time-evolution of parameter ($h = 4$): $\hat{\alpha}_1$

The details of the algorithm consisting of initialization, time update and measurement are explained. The algorithm is pointed out to be compatible with discontinuous systems. To clarify robustness of the proposed algorithm, an application to friction estimation for adaptive control is considered. In comparison with the classical UKF, simulation of using RUKF shows applaudable results.

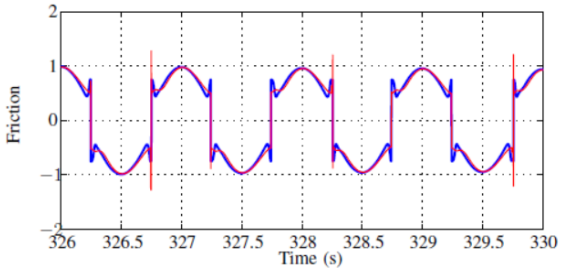

Fig. 8. Friction: black line is actual one; red line is estimation

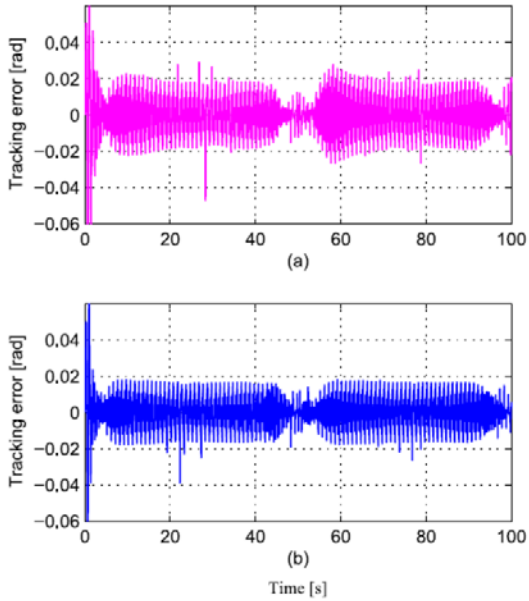

Fig. 9. Performance for bias model: (a) using UKF and (b) using RUKF with $h = 4$

REFERENCES

[1] H. Olsson, K. Astrom, C. Canudas de Wit, M. Gafvert, and P. Lischinsky, "Friction models and friction compensation", European Journal of Control, vol. 4, pp. 176-195, 1998.

[2] Q. Hui, W. M. Haddad, and S. P. Bhat, "Semistability theory for differential Inclusions with applications to consensus problems in dynamical networks with switching topology", IEEE American Control Conference, Seattle, WA, June 2008.

[3] W. M. Haddad, Q. Hui, and J. M. Bailey, "Multistability, bifurcations, and biological neural networks: A synaptic drive firing model for cerebral cortex transition in the induction of general anesthesia", IEEE Decision and Control and European Control Conf., Orlando, FL, December 2011.

[4] K. Reif, S. Gunther, E. Yaz, "Stochastic stability of the discrete-time extended Kalman filter," IEEE Trans. on Automatic Control, vol. 44, No. 4, pp. 714-728, 1999.

[5] S. J. Julier, J. K. Uhlmann and H. F. Durrant-Whyte, "A new method for the nonlinear transformation of means and covariances in filters and estimators," IEEE Trans. Automatic Control, vol. 45, pp. 477-482, Mar. 2000.

[6] R. M. van der, “Sigma-point Kalman filters for probabilistic inference in dynamic state-space models,” Ph.D., OGI School of Sci. Eng., Oregon Health and Sci. Univ., Portland, OR, 2004.
[7] S. S¨arkk¨a, “On unscented Kalman filtering for state estimation of continuous-time nonlinear system,” IEEE Trans. on Automatic Control, vol. 52, no. 9, pp. 1631-1641, 2007 [8] J. Xu,“Stochastic stability of the continuous-time unscented Kalman filter,” IEEE Proc. Decision and Control, Cancun, Mexico, 2008.
[9] S. Srang and M. Yamakita, “On the estimation of systems with discontinuities using continuous-discrete unscented Kalman filter,” IEEE American Control Conference, Portland, OR, 2014. Fig. 9. Performance for bias model: (a) using UKF and (b) using RUKF with h = 4
[10] R. Rengaswamy, S. Narasimhan, and V. Kuppuraj, “Receding-horizon nonlinear Kalman (RNK) filter for state estimation,” IEEE Trans. On Automatic Control, vol. 58, no. 8, pp. 2054-2059, 2013.
[11] S. S¨arkk¨a and J. Hartikainen, “On Gaussian optimal smoothing of nonlinear state space models,”IEEE Trans. on Automatic Control, vol. 55, no. 8, pp. 1938-1941.
[12] T. Pei, J. Long, Z. Li, Y. Zhou and Y. Choi, “A fixed-lag unscented Rauch-Tung-Striebel smoother for non-linear dynamic state estimation,” Int. J. Digital Content Technology and its Applications, vol. 7, no. 2, pp. 769-777, 2013.
[13] S. Srang, and M. Yamakita, “Adaptive friction compensation for a position control system with Stribeck friction using hybrid unscented Kalman filter,” Int. J. Information and Commumication Technology, vol. 5, No. 3, pp. 283-295, 2013.
[14] H. K. Khalil, “Nonlinear systems,” Prentice Hall, pp. 552-553, 2000.
[15] P. T. Piiroinen and Y. A. Kuznetsov, “An event-driven method to simulate Filippov systems with accurate computing of sliding motions,” CM Trans. on Mathematical Software, Vol. 34, no. 3, 2008.
[16] R. R. Laura, R. Ashok, and T. Jennifer,“Adaptive friction compensation using extended Kalman-Bucy filter frcition estimation,” Control Engineering Practice, vol. 9, no. 2, pp. 169-179, Feb 2001